Turbulence-Flame Interaction and Formation of Distributed Flame

Alexei Y. Poludnenko, Vadim N. Gamezo, Elaine S. Oran

Laboratory for Computational Physics and Fluid Dynamics
Naval Research Laboratory, Washington, DC, USA

In this work we study interaction of driven intense Kolmogorov turbulence with flames and the formation of a distributed flame. Turbulence-flame interaction is modeled using the fixed-grid massively parallel code Athena-RDX, the reactive-flow extension of the magnetohydrodynamic code Athena [1]. It employs fully unsplit corner transport upwind scheme which uses PPM spatial reconstruction in conjunction with the HLLC Riemann solver to achieve 3rd-order accuracy in space. The multidimensional coupling and low dissipation properties of this scheme are critical for minimizing numerical inaccuracies such as poor angular-momentum conservation, numerically induced anisotropies, suppression or enhancement of high-k components of the spectrum, etc.

We solve the Navier-Stokes equations with thermal conduction, molecular species diffusion, and energy release that control propagation of the laminar flame. The equation of state is that of an ideal gas and the chemical source term describes first-order Arrhenius kinetics. We consider stoichiometric CH_4/air [2] and H_2/air [3] mixtures with reaction model parameters listed in Table 1.

Turbulence driving is implemented via a spectral method. In it Fourier transforms of velocity perturbations $\delta\mathbf{u}$ are initialized with random amplitudes and phases with the Gaussian deviation. The injection energy spectrum is superimposed on the Fourier transforms of the velocity perturbations. The non-solenoidal component is projected out to ensure that the resulting perturbations are divergence-free, i.e. $\nabla \cdot \delta\mathbf{u} = 0$. An inverse Fourier transform is performed to obtain the velocity perturbation field in

Table 1: Reaction Model Parameters

	CH_4/air	H_2/air	Definition
T_0	298 K	293 K	Initial temperature
P_0	1.01×10^6 erg/cm^3	1.01×10^6 erg/cm^3	Initial pressure
ρ_0	1.1×10^{-3} g/cm^3	8.73×10^{-4} g/cm^3	Initial density
γ	1.197	1.17	Adiabatic index
M	27 g/mol	21 g/mol	Molecular weight
A	1.64×10^{13} cm^3/g·s	6.85×10^{12} cm^3/g·s	Pre-exponential factor
Q	67.55 RT$_0$	46.37 RT$_0$	Activation energy
q	39.0 RT$_0$ / M	43.28 RT$_0$ / M	Chemical energy release
κ_0	6.25×10^{-6} g/s·cm·K$^{0.7}$	2.9×10^{-5} g/s·cm·K$^{0.7}$	Transport constant
D_0	6.25×10^{-6} g/s·cm·K$^{0.7}$	2.9×10^{-5} g/s·cm·K$^{0.7}$	Transport constant

Table 2: Summary of Presented Runs

Run	Mixture	L, cm	Domain	L/l_L	$l_L/\Delta x$	ε, erg/cm^3/s	v_F, cm/s	v_F/S_L
a	CH_4/air	0.672	$128 \times 128 \times 1024$	16	8	2.5×10^9	4570	120
b	CH_4/air	0.672	$128 \times 128 \times 1024$	16	8	2.5×10^8	2121	56
c	CH_4/air	0.672	$128 \times 128 \times 512$	16	8	7.4×10^5	305	8
d	H_2/air	0.384	$128 \times 128 \times 1024$	11	8	2.5×10^8	2122	7

physical space. Resulting velocity perturbations are normalized to ensure the desired total energy injection rate. The method does not produce any large-scale anisotropies and it allows one to obtain the 5/3 slope in the inertial range even in the very low resolution runs. The saturated value of the kinetic energy density in the system is also fairly insensitive to the resolution.

We model the interaction of methane and hydrogen flames with driven isotropic and homogeneous Kolmogorov turbulence of varying intensity. Key parameters of presented runs are summarized in Table 2. Here L is the domain width, l_L is the laminar flame width, Δx is the cell size, ε is the kinetic energy injection rate, v_F is the turbulent velocity at the scale l_L, and S_L is the laminar flame speed.

The simulations results show that a distributed flame forms for sufficiently large turbulent velocities at the scale of laminar flame width, namely typically for $v_F/S_L > 50$. Values of $v_F/S_L < 10$ result in corrugated flamelets (see Fig. 2). A distributed flame represents a burning front in which thermal transport is mediated by turbulent thermal conduction and in which fuel and product are clearly separated in a manner similar to the planar laminar flame (see Fig. 4). The resulting flame is wider and faster than the laminar flame, however it shows smooth structure similar to that of the laminar flame (see Fig. 1).

We find that the Gibson scale serves as a poor indicator of the onset of the distributed flame. The Gibson scale in runs c and d was $\approx$ 1000 times smaller than the laminar flame width, yet those runs remained in the flamelet regime.

Finally, the formation of a distributed flame in mixtures with high laminar flame speeds, such as $H2/air$, is extremely difficult with subsonic turbulence. For hydrogen, $v_F/S_L = 50$ would require turbulent velocities $v_F \approx 150$ m/s (or $\approx$ Mach 0.5) at the scale of 0.3 mm.

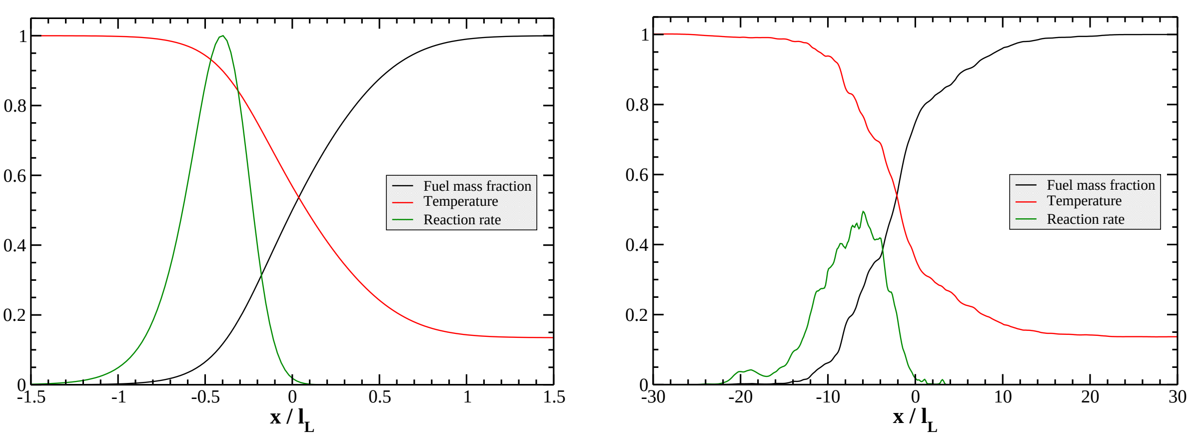

Figure 1: *Left:* Structure of the laminar flame in stoichiometric CH_4/air mixture. *Right:* Structure of the distributed flame (run b). Structure of the distributed flame is shown for the quasi-steady-state regime when flame width and energy generation rate (see Fig. 3) have reached saturated state. Temperature and reaction rate are normalized by maximum laminar flame values.

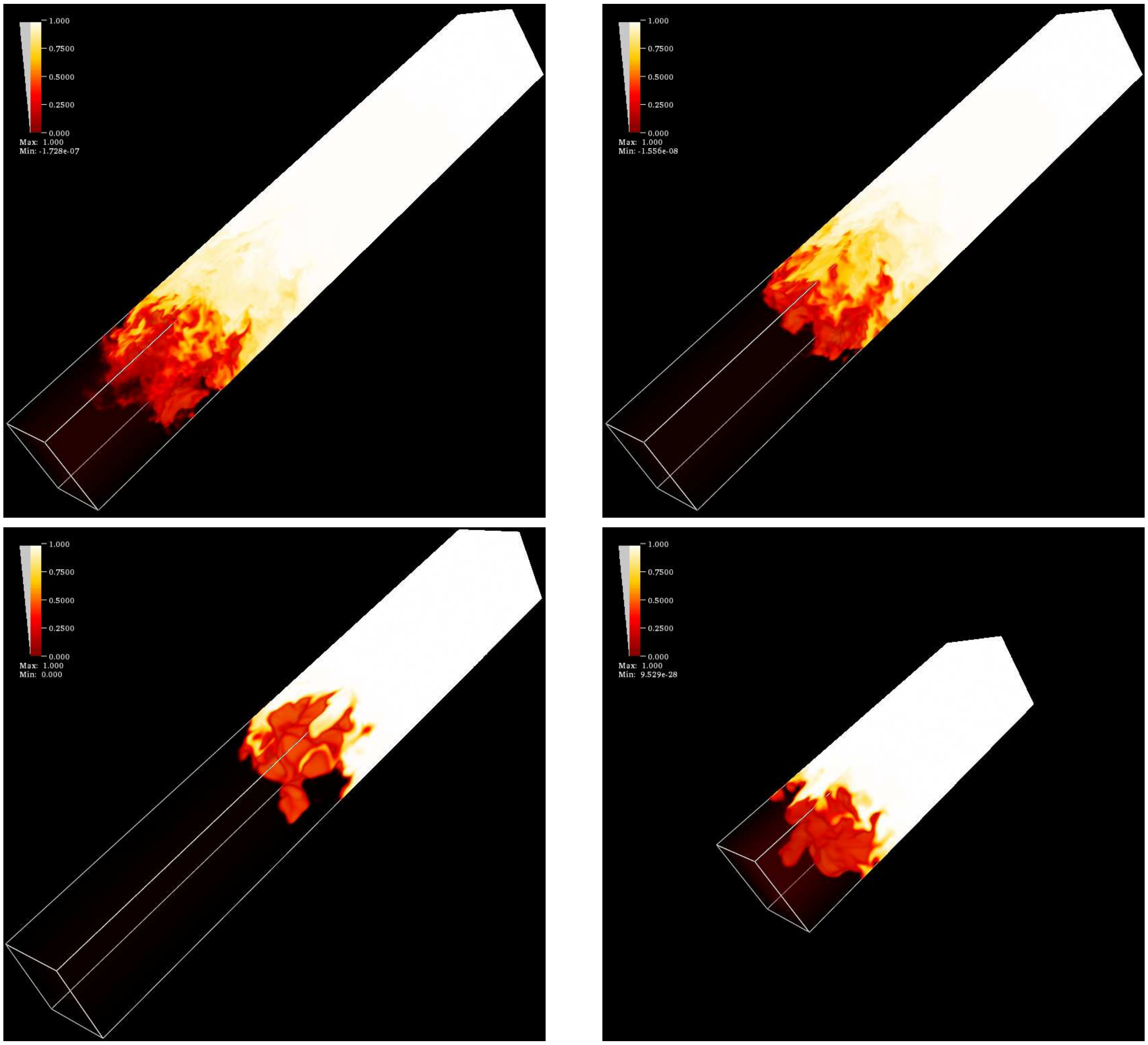

Figure 2: Volume rendering of fuel mass fraction in the domain for runs a, b, c, and d (from upper left corner clockwise). Runs a and b produced a distributed flame, while runs c and d produced a corrugated flamelet. Opacity map used for volume rendering is shown in the legend.

References

[1] Stone J.M., Gardiner T.A., Teuben P., Hawley J.F., Simon J.B. (2008). Athena: a New Code for Astrophysical MHD. Astrophys. J. Supp. 178:137

[2] Kessler D.A., Gamezo V.N., Oran E.S., Zipf R.K. (2009). Simulation of Deflagration-to-Detonation Transition in Premixed CH_4–Air in Large-Scale Channels with Obstacles. AIAA Paper AIAA-2009-0439, American Institute of Aeronautics and Astronautics, Reston, VA.

[3] Gamezo V.N., Ogawa T., Oran E.S. (2008). Flame Acceleration and DDT in Channels with Obstacles: Effect of Obstacle Spacing. Comb. Flame. 155:302

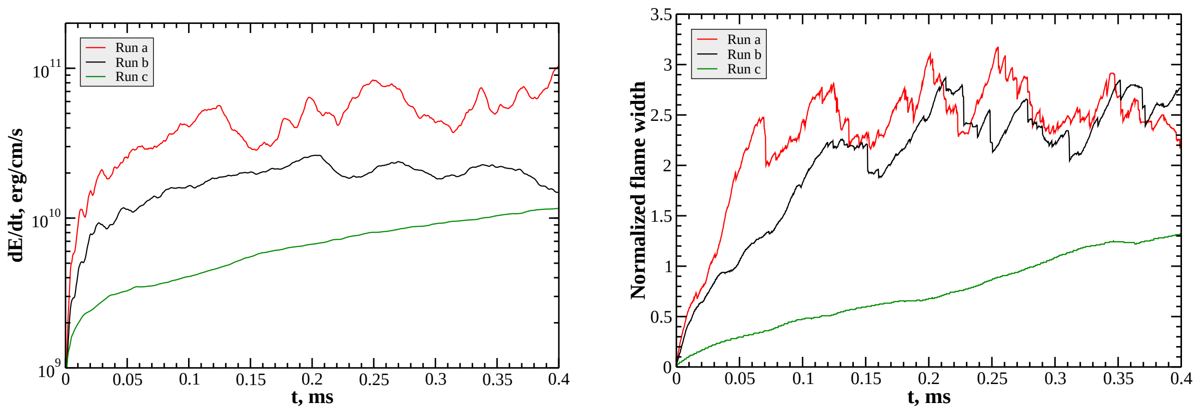

Figure 3: *Left:* Energy generation rate by the flame normalized by the domain cross section. *Right:* Flame width normalized by domain width L.

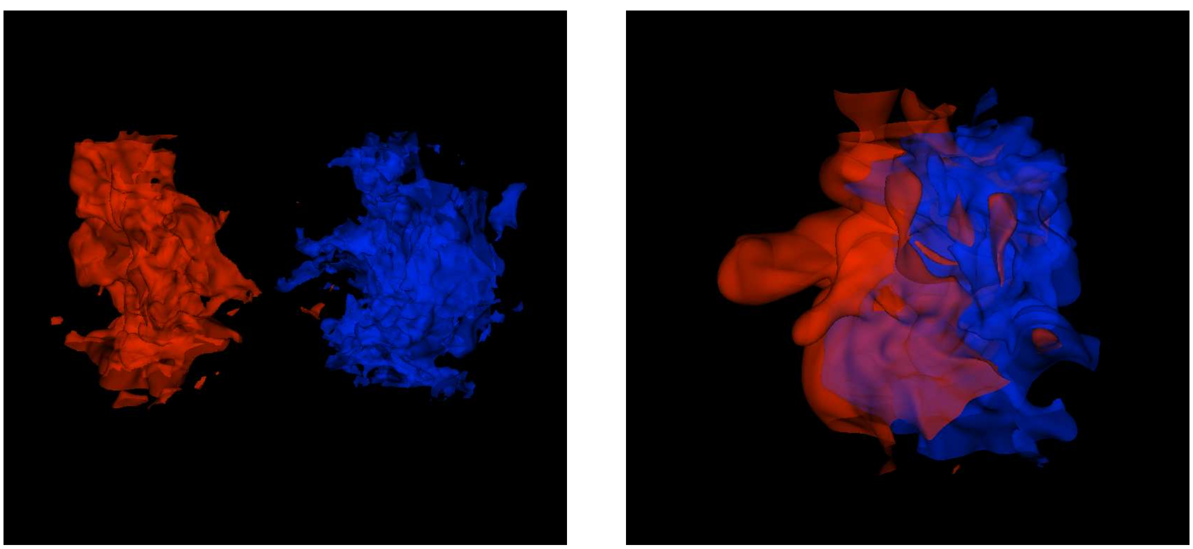

Figure 4: Isosurfaces of the fuel mass fraction c = 5% (red) and c = 95% (blue) for the distributed flame (left panel, run b) and corrugated flamelet (right panel, run c). Left and right panels correspond to the flame shown in top right and bottom right panels of Fig. 2.